INSTITUTE OF PHYSICS PUBLISHING NANOTECHNOLOGY
Nanotechnology **15** (2004) 833–838 PII: S0957-4484(04)70268-8

Alumina nanotemplate fabrication on silicon substrate

N V Myung[1,3], J Lim[2], J-P Fleurial[2], M Yun[2], W West[2] and D Choi[2]

[1] Department of Chemical and Environmental Engineering, University of California, Bourns Hall B353, 900 University Avenue, Riverside, CA 92521, USA
[2] Jet Propulsion Laboratory, California Institute of Technology, Pasadena, CA 91109, USA

E-mail: myung@engr.ucr.edu

Received 7 October 2003
Published 26 April 2004
Online at stacks.iop.org/Nano/15/833
DOI: 10.1088/0957-4484/15/7/021

Abstract

Alumina nanotemplates integrated on silicon substrate with pore diameters of 12–100 nm were prepared by galvanostatic (constant current) anodization. High current density (e.g. 100 mA cm^{-2}) promoted a highly ordered hexagonal pore structure with fast formation rate independent of anodizing solution. Alumina formation rates of 2000 and 1000 nm min^{-1} were achieved at current densities of 100 and 50 mA cm^{-2}, respectively. These rates were approximately two orders of magnitude greater than other reports in the literature.

Different electrolytes of sulfuric acid (1.8–7.2 M), oxalic acid (0.3 M) and mixed solutions of sulfuric and oxalic acids were evaluated as anodizing solutions. At fixed current density, sulfuric acid promoted smaller pore diameter with lower porosity than mixed acids and oxalic acid. The *I–V* characteristics of aluminium anodization show the measured voltages at given current densities strongly depend on solution composition, operating temperature, and bath agitation.

The pore diameter of the silicon-integrated alumina nanotemplate varied linearly with measured voltage with a slope of 2.1 nm V^{-1}, which is slightly smaller than reported data.

1. Introduction

The development of low-dimensional nanostructured materials has been the focus of research and development over the past several decades due to the enhancement in electronic, optical, and magnetic properties that occurs when electrons are strongly confined in one, two, or three dimensions. Anodized alumina is a key template material for fabrication of nanostructured materials, because it can provide large-area, nanometre-sized structures with high aspect ratios and can be fabricated inexpensively and reliably. Unlike track-etched membranes, the anodized alumina has pores with little or no tilt with respect to the surface normal, resulting in an isolating, non-connecting pore structure [1]. Anodized alumina is electrically insulating (10^{18} Ω cm^{-1}), optically transparent over a wide energy band, chemically stable, and compatible with CMOS processes [2]. A variety of nanostructured metals, metal oxides, polymers, and semiconductors have been fabricated using anodized alumina and have been applied to various electronic, optoelectronic, magnetic, and energy storage devices [3–5].

Studies of self-ordering alumina were originally initiated with the use of pure aluminium foil. Masuda *et al* found that a highly ordered honeycomb structure with an almost ideal hexagonal arrangement could be obtained over relatively large areas in oxalic acid [6] and sulfuric acids [7]. In both sulfuric and oxalic acid solutions, Masuda *et al* [6, 7] reported that long anodizing time and a constant appropriate anodizing potential improved the regularity of the cell arrangement. Even though there is approximately a factor of two volume expansion from aluminium to alumina, the thickness of alumina after anodizing can be much thinner than the aluminium thickness at slow anodizing rates, because of the chemical dissolution of alumina during anodization. The dissolution rate is a function of anodizing solution composition and operating temperature.

[3] Author to whom any correspondence should be addressed.

Masuda *et al* found that in sulfuric acid highly ordered alumina structures were obtained at 25 and 27 V. The anodizing solution and operating temperature were 0.3–0.5 M H_2SO_4 and 0–10 °C, respectively. The alumina formation rate was highly dependent on the applied voltage: film growth rates of 17 and 56 nm min^{-1} were reported at 20 and 27 V in sulfuric acid, respectively [7]. Stable anodization potentials above 27 V were difficult to maintain due to the occurrence of pitting on the surface. The concentration of the sulfuric acid and temperature of the solution did not clearly affect the self-ordering of the cell arrangement [7]. They also developed ordered hexagonal, square, and triangular alumina nanotemplates by pre-texturing the aluminium surface with moulding processes [8–10]. Liu *et al* [11] used a focused ion beam pre-patterned aluminium surface to fabricate ordered alumina nanotemplates. Sun and Kim [12] used holographically patterned aluminium films to form ordered, single-domain alumina nanotemplates.

Gosele's group [13, 14] studied the self-ordering alumina nanotemplate using sulfuric, oxalic, and phosphoric acids and observed that the best ordered periodic arrangements were observed when the volume expansion of the aluminium during the oxidation was about 1.4, which was independent of the electrolyte. Stirring had a great influence on the ordering of the pore structure and the authors observed that non-ordered alumina layers formed with 40 V in 0.3 M oxalic acid without stirring. They also showed the pores start growing at the upper surface at almost random positions, while nearly perfectly ordered densely packed hexagonal structures could be observed at the bottom of the layers.

Compared to aluminium foil, aluminium thin films provide controlled thickness of the alumina nanotemplate by varying the aluminium thickness, and most importantly it can be directly integrated with silicon electronic devices [2].

Das and McGinnis [2] fabricated alumina nanotemplates on silicon substrates by anodizing vacuum-processed aluminium in sulfuric acid. Cai *et al* [15] produced alumina nanotemplates on SiO_2 and Si substrates using oxalic acid and observed that the long-range order of alumina was improved by thermally annealing the starting evaporated aluminium films prior to anodizing. Yang *et al* [16] fabricated anodized alumina on Au/Si substrates using sulfuric acid and grew CdS nanowires. Shingubara *et al* [17] used anodized alumina as a mask to produce nano-hole arrays on silicon substrates. For all these experiments, anodizing conditions followed those of Masuda's work, which is a very long and slow anodizing process.

Despite the utility of alumina nanotemplates fabricated directly on silicon substrates for the synthesis of nano-engineered structures integrated with electronic devices, there is a dearth of reports of systematic studies to control pore dimensions and to improve processing conditions. In this paper, silicon alumina nanotemplates with controlled pore dimensions integrated on silicon were systematically investigated by studying the effect of anodizing solution composition and operating conditions on the alumina pore structure.

2. Experimental details

The aluminium thin film (5.5 μm thick) substrates were prepared by e-beam evaporating aluminium on highly doped silicon wafers. Prior to e-beam evaporation of the aluminium layers, 200 Å thick Ti layers were evaporated onto the silicon substrate to serve as adhesion layers.

Three different electrolytes (sulfuric acid, oxalic acid, and mixed sulfuric and oxalic acids) were used to determine their effect on the alumina pore structure. For sulfuric acid baths, the concentrations were varied from 1.8 to 7.2 M. For oxalic acid baths, the concentrations were fixed at 0.3 M. For mixed sulfuric and oxalic acid baths, the oxalic acid concentration was fixed at 0.3 M while sulfuric acid concentrations were varied from 0.18 to 0.45 M. Aluminium or platinum coated titanium were used as cathodes. In most experiments, the anodizing process was kept at 25 °C while rapidly stirring the bath.

A two-step anodization process was used to fabricate the ordered alumina nanotemplates on silicon substrates. Typically, the first anodization process was conducted to anodize the top 1 μm of the aluminium thin films. The anodizing time was dependent on the current density. For example, the anodizing times were 30 s at 100 mA cm^{-2} and 60 s at 50 mA cm^{-2}. The first anodized alumina layer was then selectively removed by immersing in 4 vol.% CrO_3 + 10 vol.% H_3PO_4 for 12 h at 25 °C. The concave texture of the Al surface, which formed by selective removal of the film after the first anodizing step, was used to induce the ordered formation of pores even at the initial stage of anodization in the second step.

The second anodization step was kept at the same speed as the first anodization step and lasted until the aluminium film was completely converted to alumina. The pore structures can be further adjusted by pore widening and pore shrinking. For example, pore widening and barrier layer removal can be performed in phosphoric acid at 35 °C (see reference [13]) and pores can be shrunk by converting alumina (Al_2O_3) to aluminium oxy-hydroxide (Al(O)OH) in boiling water [18]. The schematics of a two-step anodization process are shown in figure 1.

3. Results and discussion

The I–V characteristics of aluminium anodization were measured to qualitatively examine the effect of various anodizing variables (e.g. current density, solution compositions, and operating temperature) on the anodizing rate and stability of anodizing processes. Figure 2 shows the effect of anodizing solution composition (figure 2(a)) and operating temperature (figure 2(b)) on aluminium anodization. As expected, the I–V characteristics of aluminium thin film anodization were strongly influenced by solution composition and operating conditions. In general, the potential (voltage) initially increased slowly with an increase in applied current densities, followed by a rapid increase in the current density without significant change in voltage. At a given applied current density, the measured voltage from oxalic acid was higher than sulfuric acid. In the case of the mixed sulfuric and oxalic solution, the measured voltage was between the measured voltages from sulfuric acid and oxalic acid solutions. The measured voltages decreased with increasing sulfuric acid concentration in sulfuric acid solution. The measured voltage decreased with increasing temperature similar to reported literature data on high purity (99.99%) aluminium [18]. It became difficult to

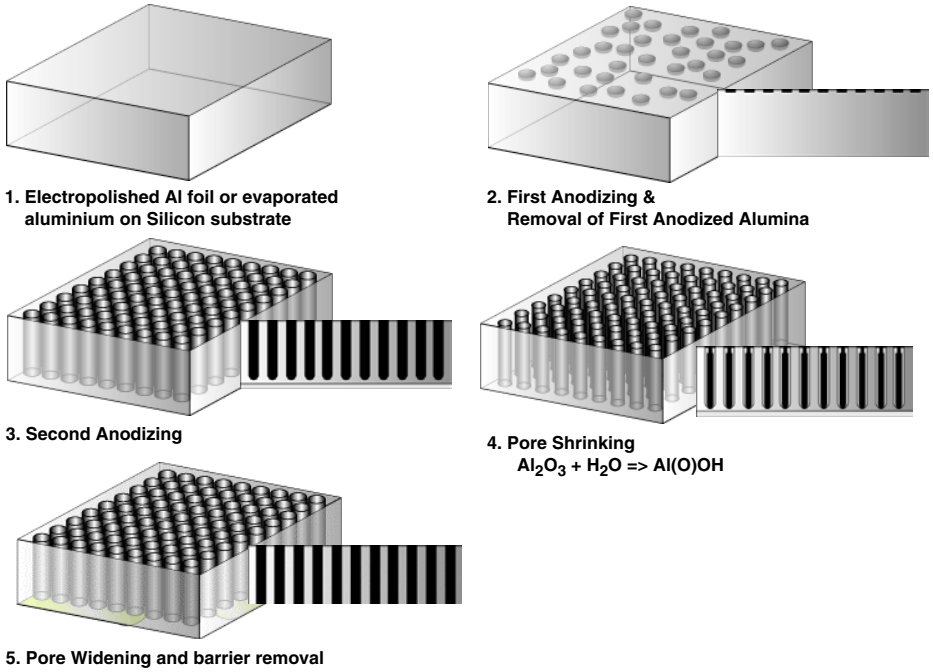

Figure 1. The schematics of a two-step anodization process.

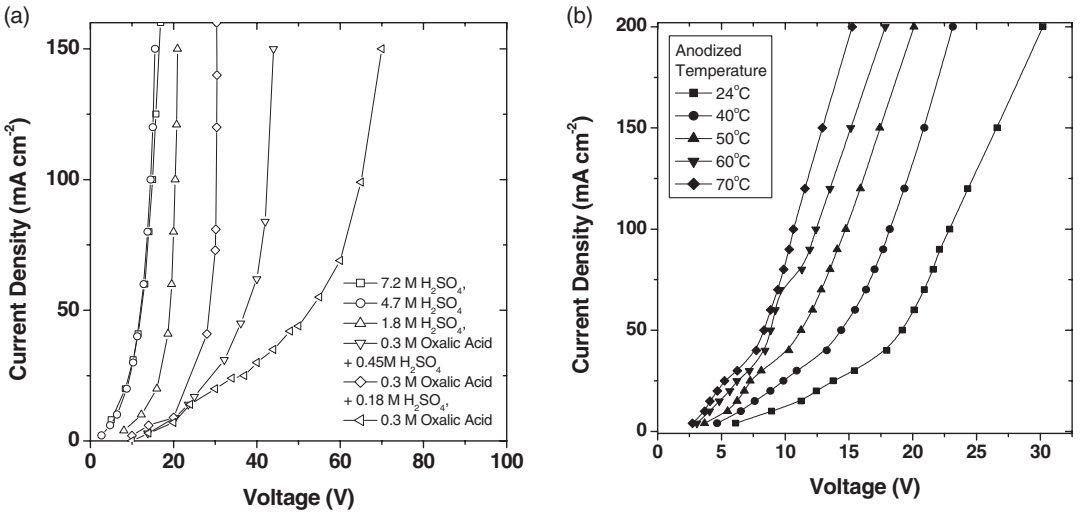

Figure 2. The I–V characteristics of aluminium anodization: (a) the effect of solution composition at room temperature, and (b) voltage, current and operating temperature relationship in 7.2 M H_2SO_4.

achieve a high current density with fixed voltage (potentiostatic) because small fluctuations in the voltage caused large variations in current density. However, high current density can be achieved by galvanostatic (constant current) control.

Since the pore structure including pore dimensions and porosity of the alumina nanotemplate is dependent on the applied voltage [18], an alumina nanotemplate with controlled pore dimensions can be achieved by altering the solution composition and operating temperature at fixed current density. Figure 3 displays the SEM micrograph of an anodized alumina nanotemplate on a silicon substrate from sulfuric acid baths at controlled current density and fixed temperature of 25 °C. As predicted from the I–V curves, pore structures were strongly dependent on solution composition. For example, alumina nanotemplates with pore diameter of 35 nm were fabricated from 1.8 M sulfuric acid with current density of 100 mA cm^{-2} (figure 3(a)). Alumina nanotemplates with pore diameter of 17 nm were fabricated from 4.7 M sulfuric acid (figure 3(b)) with current density of 100 mA cm^{-2} and 7.2 M sulfuric acid with current density of 50 mA cm^{-2} (figure 3(c)). Alumina nanotemplates with pore diameter of 12 nm were fabricated from 7.2 M sulfuric acid with current density of 100 mA cm^{-2} (not shown). However, many defects were observed from these samples. Porosity decreased from 31% to 15% with increasing sulfuric acid concentration at fixed current density.

Figure 4 shows the SEM micrographs of alumina nanotemplates anodized from mixed sulfuric and oxalic baths (figures 4(a) and (b)) and oxalic baths (figure 4(c)) at 25 °C. At fixed oxalic acid concentration (i.e. 0.3 M), the pore diameter of alumina nanotemplates decreased from 106 to 47 nm with

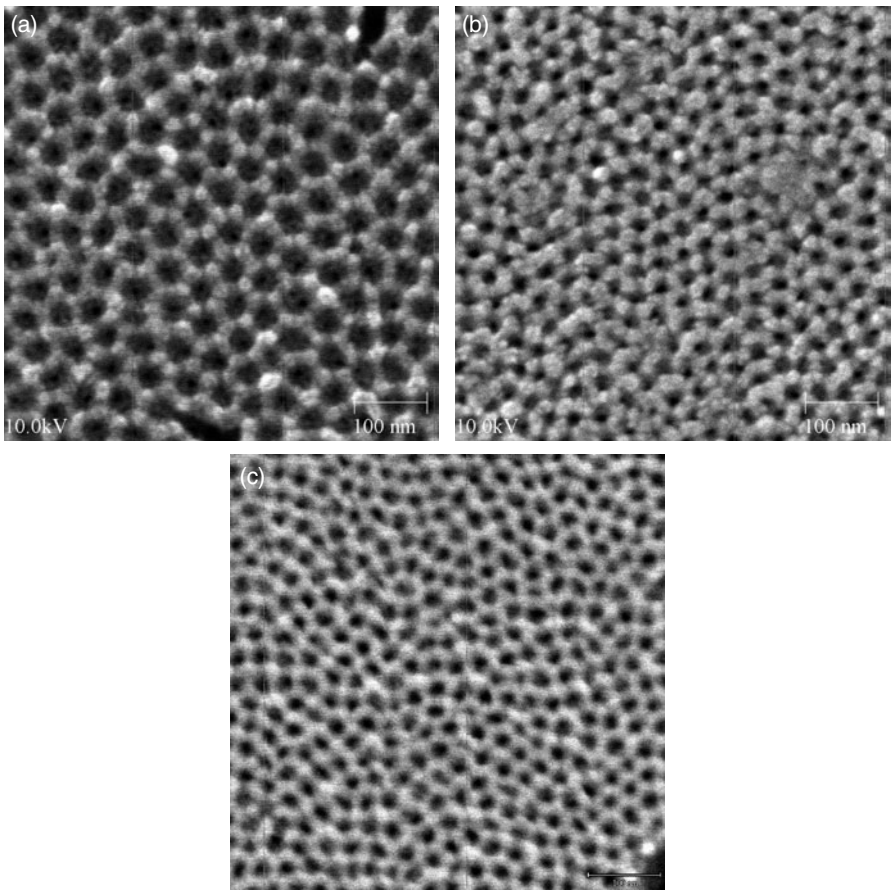

Figure 3. Top views of anodized alumina nanotemplate on a silicon substrate from sulfuric acid. (a) 1.8 M sulfuric acid, CD = 100 mA cm^{-2}, pore diameter of 35 nm, (b) 4.7 M sulfuric acid, CD = 100 mA cm^{-2}, pore diameter of 17 nm, and (c) 7.2 M sulfuric acid, current density = 50 mA cm^{-2}, pore diameter of 17 nm with rapid agitation: operating anodization temperature was 25 °C.

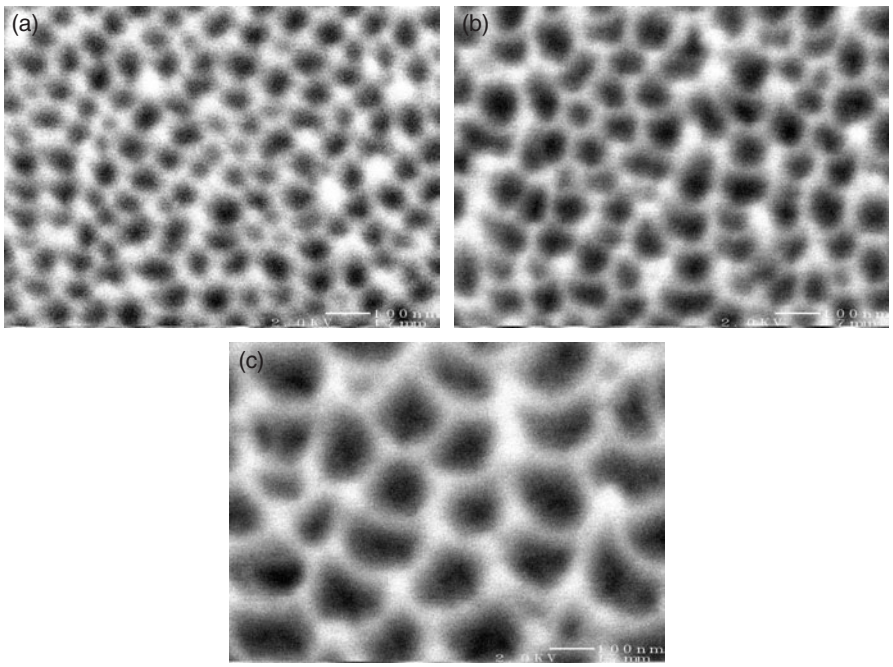

Figure 4. Top view of anodized alumina nanotemplate from mixed sulfuric and oxalic acid baths and oxalic acid baths. (a) 0.3 M oxalic acid + 0.45 M sulfuric acid, pore diameter of 47 nm, CD = 100 mA cm^{-2}, (b) 0.3 M oxalic acid + 0.18 M sulfuric acid, pore diameter of 57 nm, CD = 100 mA cm^{-2}, and (c) 0.3 M oxalic acid with pore diameter of 106 nm, CD = 50 mA cm^{-2}: operating anodization temperature was 25 °C.

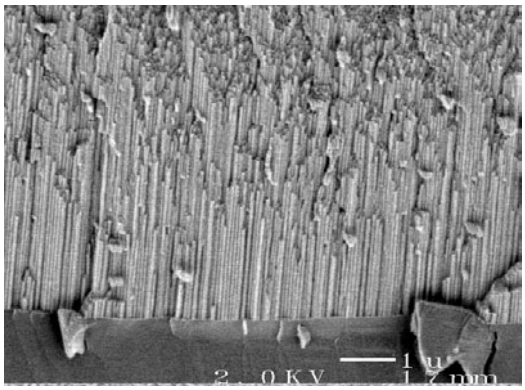

Figure 5. Cross-sectional view of anodized alumina nanotemplate on a silicon substrate from 1.8 M sulfuric acid. CD = 100 mA cm^{-2}; operating anodization temperature was 25 °C.

addition of 0.45 M sulfuric acid. Porosity also decreased from 63% to 43% with addition of 0.45 M sulfuric acid. Unlike the alumina nanotemplates from sulfuric acid baths, oxalic acid baths produced less ordered alumina nanotemplates with larger pore diameter distribution. Figure 5 shows cross-sectional micrographs of an alumina nanotemplate integrated on a silicon substrate. As shown in this micrograph, the alumina nanotemplate was readily integrated on the silicon substrates. Most of the ordered alumina nanotemplates were fabricated with little or no tilt with respect to the surface normal, resulting in an isolating, non-connecting pore structure observed for 1.8 M sulfuric acid at 100 mA cm^{-2} conditions (figures 3(a) and 5). The titanium film enhanced the adhesion between the silicon substrate and alumina. In the absence of the titanium adhesion layer, the alumina nanotemplates delaminated from the substrate.

Figure 6 plots the experimentally measured pore diameters and porosity of the alumina nanotemplates as a function of measured voltages for various electrolyte solutions. The pore diameter varied linearly with the measured voltage with a slope of 2.1 nm V^{-1}, which is slightly smaller than obtained in previous reports for bulk aluminium (2.2 and 2.77 nm V^{-1}) [18]. The difference may be attributed to the purity of the film and the number of film defects. The porosity of alumina increased monotonically with increasing voltage, but the porosity can also be altered after post-treatments (e.g. pore widening and pore shrinking).

The formation rate was determined by measuring the alumina nanotemplate thickness at fixed anodizing time. Applied current density was the most important factor which determined the alumina formation rate. For example, formation rates of 1000–2000 nm min^{-1} were achieved at applied current density of 50 and 100 mA cm^{-2}, respectively. These rates were approximately two orders of magnitude greater than other reports in the literature [6, 7] because of the high applied current density. The anodizing solution compositions and operating temperatures can also influence the formation rate because of the chemical dissolution of alumina during anodization is strongly dependent on the solution composition and operating temperature.

4. Summary

Alumina nanotemplates were successfully fabricated and directly integrated on silicon substrates. The pore diameter and the length could be controlled by adjusting anodizing conditions including solution compositions, operating temperature, and the thickness of the e-beam evaporated aluminium. Pore diameters of 12–100 nm were fabricated with a formation rate of 1000–2000 nm min^{-1}. Sulfuric acid produced the smallest pore structures, followed by mixed sulfuric and oxalic acids and then oxalic acid.

Acknowledgments

This research was performed at the Jet Propulsion Laboratory, California Institute of Technology, under a contract with the National Astronautics and Space Administration. The authors would like to thank Ron Ruiz for his SEM work.

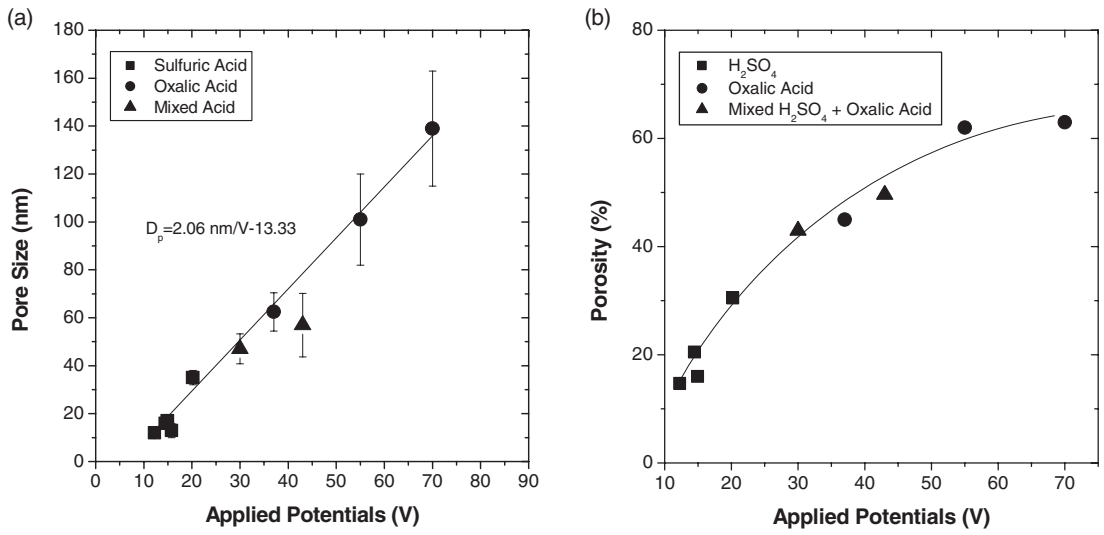

Figure 6. Pore diameters and porosity of alumina nanotemplate as a function of electrolyte solution at 25 °C. Current density was fixed at 100 mA cm^{-2}.

References

[1] Huczko A 2000 *Appl. Phys.* A **70** 365–76
[2] Das B and McGinnis S P 2000 *Appl. Phys. A. Mater.* **71** 681–8
[3] West W, Myung N V, Whitacre J F and Ratnakumar B V 2004 *J. Power Sources* **126** 203
[4] Fleurial J-P, Synder G J, Myung N V, Huang C K, Herman J, Ryan M A and Whitacre J 2002 *Proc. Electrochem. Soc. PV2002-25* pp 203–14
[5] Myung N V, Park D-Y, Schwartz M and Nobe K 2000 *Proc. Electrochem. Soc.* **PV2000-25** 333–44
[6] Masuda H and Fukuda K 1995 *Science* **268** 1466–8
[7] Masuda H, Hasegwa F and Ono S 1997 *J. Electrochem. Soc.* **144** L127–30
[8] Masuda H, Yamada H, Satoh M and Asoh H 1997 *Appl. Phys. Lett.* **71** 2770–2
[9] Masuda H, Asoh H, Watanabe M, Nishio K, Nakao M and Tamamura T 2001 *Adv. Mater.* **13** 189–92
[10] Asoh H, Nishio K, Nakao M, Yokoo A, Tamamura T and Masuda H 2001 *J. Vac. Sci. Technol.* B **19** 569–72
[11] Liu C Y, Datta A and Wang Y L 2001 *Appl. Phys. Lett.* **78** 120–2
[12] Sun Z and Kim H K 2002 *Appl. Phys. Lett.* **81** 3458–60
[13] Li A P, Muller F, Birner A, Nielsch K and Gosele U 1998 *J. Appl. Phys.* **84** 6023–6
[14] Jessensky O, Muller F and Gosele U 1998 *J. Electrochem. Soc.* **145** 37735–40
[15] Cai A, Zhang H, Hua H and Zhang Z 2002 *Nanotechnology* **13** 627–30
[16] Yang Y, Chen H, Mei Y, Chen J, Wu X and Bao X 2002 *Solid State Commun.* **123** 279–82
[17] Shingubara S, Okino S, Murakami Y, Sakaue H and Takahagi T 2001 *J. Vac. Sci. Technol.* B **19** 1901–4
[18] Wernick S and Pinner R 1964 *The Surface Treatment and Finishing of Aluminum and its Alloys* (Teddington: Robert Draper Ltd) chapter 6